

## Highly perturbed states of barium in a static electric field

Kenneth A. Bates, Jumpei Masae, Camelia Vasilescu, and Douglass Schumacher

*The Ohio State University, Columbus, Ohio 43210*

(Received 30 March 2001; published 6 August 2001)

The spectrum of nominally bound states in barium in an electric field has been measured in a region where singly excited Rydberg states are heavily perturbed by a doubly excited state. Wave-packet and recurrence map analyses are performed and significant deviations are observed from the standard one-electron picture due to the more complex core.

DOI: 10.1103/PhysRevA.64.033409

PACS number(s): 32.60.+i, 03.65.Sq

### I. INTRODUCTION

We have studied the Stark spectrum of barium in the vicinity of the  $5d7d\ ^1D_2$  doubly excited state. This state is inserted into the  $6snd\ ^1,3D_2$  Rydberg series near  $n=26$  causing the states in this region to have mixed singly and doubly excited character. It is possible to excite to these states in proportion to their amount of singly or doubly excited character, and we have done the latter. Classically, we expect the dynamics of both characters to be present, but this excitation method selects an interesting set of initial conditions. We have analyzed the resulting spectra in terms of both wave-packet evolution and the actions of the contributing periodic orbits. The wave-packet analysis shows behavior qualitatively similar to that in one-electron systems, but on time scales that are too long to be described using one-electron scaling laws. For example, the observed Kepler time is roughly 50% larger than predicted by  $2\pi n^{*3}$ , where  $n^*$  is the quantum defect-corrected principal quantum number. We show that the difference can be explained by two factors. The first is the increased anharmonicity in this system caused by the intrusion of the  $5d7d\ ^1D_2$  state, henceforth referred to as the perturber, into the Rydberg series. The second is an increase of the Rydberg orbit time because of the strong probability of capture by the core and creation of a doubly excited state. In an analogous way, the recurrence map for this system has a fairly simple appearance, but the peaks, at large-magnitude-scaled energy, are shifted from their one-electron locations. This is due to the energy dependence of the quantum defect for the Rydberg series and is another manifestation of the more complicated barium core.

The reintroduction of classical mechanics to problems in quantum mechanics has greatly invigorated the experimental and theoretical treatment of simple systems in external fields. The problem of a one-electron atom in static electric, magnetic, or combined fields has received most of the attention [1]. In hydrogen, the Hamiltonian is well understood; simple scaling laws exist, and yet spectra can be of great complexity. In many cases, a semiclassical analysis has proven more insightful than a quantum-mechanical analysis, and features in the spectrum, when suitably transformed, can be directly associated with families of classical orbits [2]. In “one-electron” atoms such as the alkali metals the potential is no longer Coulombic near the core, and even far from the core small, but important, deviations from a Coulombic potential

occur due to the core’s polarizability. Because of this, the one-electron Hamiltonian no longer scales exactly and yet there is still considerable similarity to hydrogen. In particular, a semiclassical analysis is still possible and fruitful [3–7]. Classical orbits identified as important for hydrogen now appear in combination as well as separately. In recent times attention has turned to helium [8–10] and other “two-electron” atoms such as barium [11,12]. There are good reasons for this. The success of the new semiclassical methods demands that their generality be tested. Moreover, two-electron atoms are well-placed intermediaries between the simplicity of hydrogen and the complexity of most of the atoms in elements in the periodic table and of molecules. They can be excited to states that are still reasonably similar to those of one-electron atoms and yet also have regions where the configuration interaction is manifest, for example, as in autoionization.

### II. BARIUM

In zero field, quantum defect theory (QDT) suggests a scattering picture. This has been studied directly by observing the evolution of wave packets excited with a specific character [13]. There are several possible relevant time scales: the Kepler time, the singly-doubly excited character mixing time, and the fine-structure mixing time. These time scales were identified in theoretical and experimental studies where a wave packet was excited that initially had one character, and then the amount of singly or doubly excited character present was monitored as a function of time [13]. The time scale corresponding to the precession of the classical orbit due to the finite core size, well defined in alkalis, is difficult to define in barium for eigenstates with an energy-dependent quantum defect. Classically, we can think of a wave packet that is initially singly excited in character as an  $nd$  electron following a highly elliptical orbit. When the orbit takes the electron back to the core, it collides with the other valence electron in  $6s$  and both follow orbits with energy and angular momentum corresponding to  $5d$  and  $7d$  states. However, the electrons quickly scatter again with one returning to  $6s$  and the other to  $nd$ . In an electric field that is below the classical ionization threshold, a new time scale enters, namely, the time it takes for the orbital angular momentum of the  $nd$  electron to precess. Finally, in addition to these classical time scales, there are times scales that are quantum mechanical in nature. These characterize the time

over which a quantum wave packet can remain localized along some coordinate (not necessarily spatial) and when, if ever, it will reform once dispersed.

Several recent studies have looked at helium singly excited states and found good agreement between experiment and closed-orbit theory (COT), at least for low to moderate action [9,10]. Core effects have been identified as well as exchange effects, which dominate in some cases. By contrast, core effects are large in barium and exchange is not expected to be important. In general, implementations of COT assume a symmetric core, but this is no longer a safe assumption. Complications also arise in COT because of the  $m_l$  quantum number. The Hamiltonian can only be put in scaled form for  $m_l = 0$ . In this case, however, uphill and downhill orbits exist, which bifurcate at certain scaled energies and give rise to infinities in the theory. Finally,  $m_l$  is not a good quantum number in alkali or alkali-earth atoms, and so, in general, multiple  $m_l$  states are excited. These complexities have been manageable for the one-electron atoms studied. The infinities are avoided by the uniform approximation [14] and the difference between the zero and nonzero  $m_l$  in the semiclassical region is argued to be small. The mixture of  $m_l$ 's can be dealt with using a coherent or incoherent sum depending on the experiment. Recent studies, however, have shown that COT, as presently formulated, is less successful with a two-electron atom such as barium [11,12]. Both autoionizing and bound states have been examined, and although agreement between theory and experiment on recurrence-peak position is good, agreement on amplitude is not. The amplitude of a recurrence peak depends on a variety of factors including the stability of the contributing classical orbit, the nearness of bifurcations, and a matrix element that describes how the initial state (which is typically of mixed configuration in barium) couples to the initial outgoing wave at the semiclassical boundary. Although theory is rising to the experimental challenge, experimental work in two-electron systems clearly stands as one of the important tests for COT. We take advantage of an aspect of barium that will be useful in this regard. We excite to  $6snd\ ^1,^3D_2$  via the  $5d6p\ ^3D_1$  odd parity state, which couples to the  $6snd$  series in proportion to its energy-dependent doubly excited character [15]. This character is distributed in a relatively narrow energy range of roughly  $100\text{ cm}^{-1}$  about the perturber, comprising only a few  $n$  manifolds. This places a physical limit on the action (or, equivalently, time) resolution of this system. This system has long been a focus of study and analysis via QDT and is well understood at zero field [13]. There has been recent success describing the forced autoionization spectrum using modified QDT and a basis consisting of a large number of channels [16]. Forced autoionization using the same excitation pathway to the perturber as this work was studied experimentally via spectroscopy and an atomic streak camera as well as theoretically for several fields in the vicinity of  $1600\text{ V/cm}$  [17]. Our work focuses on behavior below and near the autoionizing limit over a wide range of field.

### III. EXPERIMENT

The apparatus used to collect the Stark data was straightforward. A resistively heated oven and an aperture were used

to generate a diffuse atomic beam of barium. The beam intersected two co-propagating pulsed laser beams (5-ns pulse width and 5-ns separation between them) at right angles between two flat-plate electrodes with plate separation 1 cm. The electrodes were used to impose a static electric field as well as to field ionize the atoms after laser excitation. The field-ionized electron current was collected through a small hole, diameter  $100\ \mu$ , in one of the plates and measured by a microchannel plate detector. One laser excited from  $6s^2 \rightarrow 5d6p\ ^3D_1$  (413 nm) and the other from  $5d6p\ ^3D_1$  to the Rydberg series (566 nm when tuned to the perturber). The wavelength of the second laser was calibrated using a state at zero field on each run, and monitored by measuring transmission through a 5-mm etalon as the wavelength was scanned. The first laser saturated the transition to the  $5d6p$  initial state and the signal was normalized by the intensity of the second laser, which was measured shot to shot. Ordinary Stark maps were measured in this way as well as scaled energy maps. A Fourier transform of the former provides a wave-packet picture of this system, whereas the transform of the latter yields information on contributing closed orbits. The scaled energy data were obtained by interpolation from the Stark map as well as collected directly. In the latter case, the electric field was varied simultaneously as the second laser was scanned so as to keep the scaled energy,  $\varepsilon = E/\sqrt{F}$ , constant. The two-electron Hamiltonian is not scale invariant, of course. The scaled energy was kept constant in the approximation that barium can be treated as a one-electron system whose nonhydrogenic character can be characterized using energy-independent quantum defects.

### IV. RESULTS

The graph in Fig. 1(a) shows the zero-field spectrum for this system, centered about the perturber energy, defined as zero (the perturber is  $41\,841.660\text{ cm}^{-1}$  above the ground state and  $193.38\text{ cm}^{-1}$  below the  $6s$  ionization limit, giving it a principal quantum number of  $n^* = 23.8$ ). The perturber character is primarily distributed through the  $^3D_2$  states below the perturber and through the  $^1D_2$  states above. The bottom graph in Fig. 1(b) plots the measured integrated absorption strength for just these states (circles), the calculated absorption strength using three-channel QDT (crosses), and a Lorentzian that was fit to the data (solid line). The lifetime of the doubly excited state as determined from this fit is  $0.58\text{ ps}$ . Figure 2 is our measured Stark map for excitation with both lasers' polarization parallel to the static field. A previous experiment using a different perturber inserted near  $n = 12$  observed that it acted almost as a spectator, not interacting strongly until high fields were reached, and then only to transition from having a quadratic shift in the field to a more linear shift [18]. Our case is different. Our spectra measure the energy dependence of the perturber character. We observe that the perturber character integrated over energy is roughly independent of field strength except at the largest fields, as one would expect. However, the applied field disperses the character over more resonances and so the peak amplitude drops. The signal is always centered about the perturber, but the degree of localization of the signal oscil-

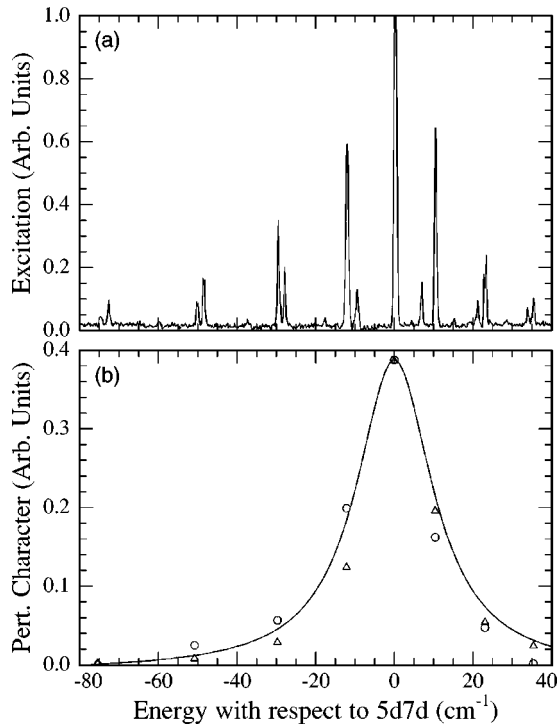


FIG. 1. (a) Zero-field excitation spectrum. Energy is given with respect to the  $5d7d \ ^1D_2$  state. (b) Integrated signal for each peak with significant perturber character (circles), calculated value (triangles), fit of data to a Lorentzian (solid line).

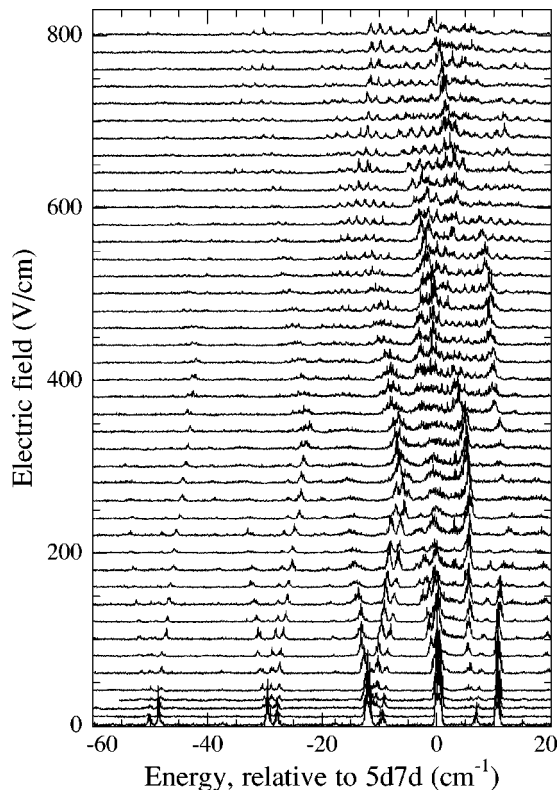


FIG. 2. Stark map for barium near the  $5d7d \ ^1D_2$  perturber.

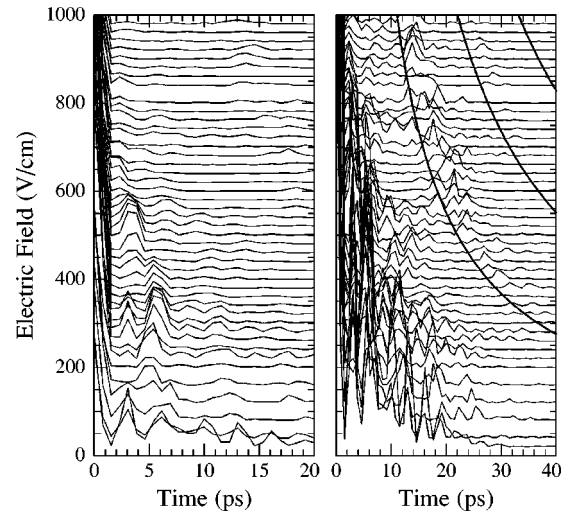


FIG. 3. Wave-packet interferograms derived from the Stark map. The right panel plots the data with the signal level multiplied by 5 as compared to the left panel to bring out the structure at longer times and higher fields. The curved dark lines indicate the one-electron Stark time and its multiples.

lates with a period of roughly 200 V/cm. The spectrum on the red side of the perturber is clearly  $m=0$  in character, with curve crossings occurring in reasonable accord with the one-electron scaling law  $1/3n^{*5}$ , which yields, for the  $6s24d$ ,  $6s25d$ , and  $6s26d$  triplet states, respectively, 399 V/cm, 319 V/cm, and 259 V/cm.

The left graph in Fig. 3 provides a wave-packet view of the system. It was obtained by masking each run in Fig. 2 with a half cycle of a cosine function centered at the zero-field perturber energy, and then taking the Fourier transform. The spacing between nodes of the cosine function was  $45 \text{ cm}^{-1}$ . The resulting plots are the autocorrelation function of the wave function of a wave packet such as might be launched by a short pulse laser whose spectrum is centered on the perturber [19]. A peak in the autocorrelation function means that the wave packet at that time resembles its state at  $t=0$ . The lowest trace, at zero field, naturally has peaks spaced every Kepler period, which by inspection is 3.0 ps. The “predicted” Kepler period using the one-electron scaling law  $2\pi n^{*3}$  is only 2.05 ps using  $n^*=23.8$ . Note that the first return alternates between 3 ps and somewhere between 5 and 6 ps every 200 V/cm. The left side of Fig. 3 shows the autocorrelation function, but over a longer range in time and with a signal magnification of 5 compared to the right side. As the field is increased, the returns quickly die out, but then recover weakly at approximately the one-electron Stark time,  $2\pi/3n^*F$ . The Stark time is the time it takes for the angular momentum vector to precess from its initial low magnitude through high values back; and the one-electron law given above is marked in the figure with a heavy solid line. The true returns are consistently “late,” and a second Stark return, also late, is suggested by the data.

Figure 4 provides yet another view of the Stark spectra. The Stark map of Fig. 2 has been interpolated to construct a recurrence map. A slice was taken across the Stark map such that the scaled energy  $\varepsilon = E/\sqrt{F}$  was kept constant, where  $E$

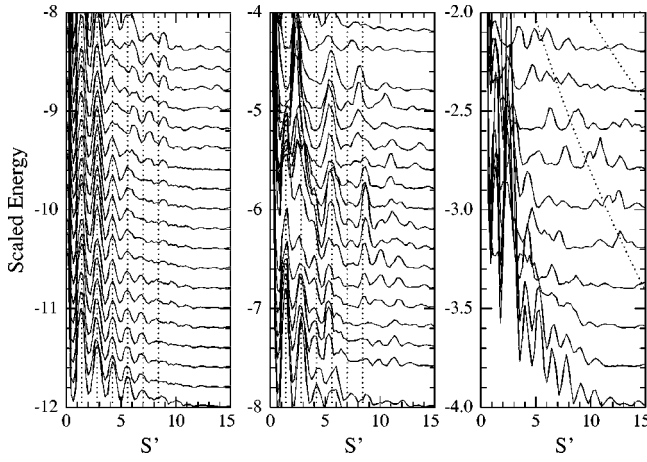


FIG. 4. Recurrence map derived from the Stark map. The first two panels show data for low- and moderate-scaled energy and the dotted lines are spaced at integer multiples of 1.4 as a guide. The last panel shows data at high-scaled energy and the signal amplitude has been multiplied by 2 compared to the other panels. The curved dotted lines indicate the predicted location for recurrences with significant amplitude assuming one-electron-like behavior.

is the energy and  $F$  the static field. This was done for various scaled energies from  $\varepsilon = -2$ , where the field is maintained so that a state at energy  $E$  just becomes unbound, to  $\varepsilon = -12$ , where the field remains well below the manifold-crossing value. After the slice, the data is still in the form of signal versus excitation energy. Following Pisharody *et al.* [20], the energy axis is converted to  $n^*$  and the data is Fourier transformed. In a one-electron system, the resulting graph will consist of recurrence peaks located at integer or half-integer values. The recurrence peaks will generally only be large near a bifurcation of the uphill or downhill orbits, or one of their repeated traversals. Figure 4 shows the results for  $-12 \leq \varepsilon \leq -2$  in three panels. The field  $F$  lies in different ranges depending on the value of  $\varepsilon$ . For this work  $\varepsilon = -12$  has  $22 \text{ V/cm} \leq F \leq 47 \text{ V/cm}$ ;  $\varepsilon = -8$  has  $50 \text{ V/cm} \leq F \leq 106$ ;  $\varepsilon = -4$  has  $199 \text{ V/cm} \leq F \leq 425$ ; and  $\varepsilon = -2$  has  $795 \text{ V/cm} \leq F \leq 1700 \text{ V/cm}$ . For  $\varepsilon$  close to  $-2$ , however, some of the signal appears as prompt ionization (before the ramped field ionization occurs) and is lost to background noise in our apparatus. Generally only modest attention is paid to large-magnitude values of  $\varepsilon$ ; however, there are features worthy of attention. The recurrence spectrum at  $\varepsilon = -12$  consists of broad peaks located at multiples of 1.4 (vertical dotted lines spaced by 1.4 are plotted as a guide in the first two panels). At these low-field values, only a single closed orbit contributes, with each traversal of this orbit giving rise to a peak at increasing action. The spacing between peaks is clearly not integer or half integer, as can be seen by looking at the peaks at larger  $S'$ . The width of the peaks is determined by the small range in energy over which there is signal. This is a characteristic of barium, not an experimental limitation. As the scaled energy is increased from  $\varepsilon = -12$ , there is a small increase in the decay of the recurrences with  $S'$  until  $\varepsilon = -9.4$  where the decay is reversed and the third and later recurrences shift to larger scaled action. The first recurrence vanishes near  $\varepsilon = -4.5$  and reappears at  $-3.3$ .

The second recurrence, on the other hand, vanishes near  $-6.5$ . The third and fifth recurrences are weak. The fourth and sixth recurrences periodically grow and decay. Finally, there is a weak second branch of recurrences at low-magnitude-scaled energy.

## V. DISCUSSION

Barium appears to live on a different time scale than the alkali atoms. Its Kepler and Stark times are both long for a given state energy, and so naturally the actions of its contributing orbits are larger. The long Kepler time can be understood from a simple argument. Every time the outermost ( $nd$ ) electron returns to the core, there is a strong probability that it will collide with the inner ( $6s$ ) electron and scatter into the degenerate  $5d7d$  doubly excited state. Eventually the reverse process occurs and one of the electrons is scattered back into an orbit consistent with  $nd$ . This effectively increases the orbital period by something like the lifetime of the doubly excited state, 0.58 ps. The  $nd$  electron, like the valence electron in an alkali metal, lives in an anharmonic potential except that the anharmonicity is larger. This increases the Kepler period by 0.29 ps, as determined by fitting the zero-field energy levels to a polynomial. Adding these times with the “base” Kepler time,  $2\pi n^{*3} = 2.05$  ps, yields 2.92 ps, roughly what we observe. In alkali metals, penetration into the relatively rigid core results in the electron speeding up due to the loss of screening. In barium, the core is less rigid and this effect is almost compensated. We expect then that all other time scales will be increased. The ratio of the scaled action,  $S'$ , of a primitive orbit of barium to that of an equivalent orbit in a one-electron system should go as the ratio of the periods, or 1.5 in this case. The observed  $S'$  is 1.4. We should not expect a *proportional* increase in the Stark time, because the static electric field quickly causes the angular momentum to precess to large values, and the core is not sampled over most of the Stark time. What we observe is a nearly fixed 2-ps shift to later times compared to the value expected for a one-electron atom. That would seem to suggest that the electron manages to go near the core roughly twice each Stark period. At first sight this appears odd since the Kepler time is essentially fixed whereas the Stark time varies by a factor of 4 over the range of data where it is observable. This is easily explained. For the fields over which we can observe the Stark time,  $F \geq 250 \text{ V/cm}$ , the angular momentum is rapidly torqued to a value greater than  $l_{core} = 2$ . This occurs in a time between 0.4 and 1.5 ps over the range of the dark curve marking the one-electron Stark return time in Fig. 3. Thus, the only times the electron sees the core are when it launches and a Stark period later. Recall, we excite to states in proportion to their doubly excited character. This corresponds to picking initial conditions such that the electron *starts* in a doubly excited configuration and must scatter into a singly excited configuration before it launches into the semiclassical region.

The starting point for most discussions of the structure in a recurrence map is the location of bifurcations of the fundamental uphill and downhill orbits and their repeated traversals. Recurrences tend to be strong in the vicinity of bi-

furcations and so they dominate the large-scale structure of the map. The two slanted dotted lines in the third graph of Fig. 4 indicate the location of these points, assuming one-electron behavior for the range of scaled action considered in this treatment [20,21]. There is indeed a cluster of peaks following the lowest curve. The observation of peaks following higher-order curves would require examination of larger actions, however, the signal falls off sharply with action and it is difficult to discern much from the noise beyond  $S' = 15$ . The large-scale structure at small-magnitude-scaled energy is similar, at least in gross detail, to that in one-electron systems. A key test of any theory will be to explain the detailed behavior of the peak locations and amplitudes. Also of interest is the structure observed in the plots at larger-magnitude scaled energy. At a minimum, we can explain some of this from the behavior of the *scaled* Stark map [21]. This is the regularized version of Fig. 2 from which the recurrence map was derived via Fourier transform. For example, at scaled energies between roughly  $-7$  and  $-5.5$ , the manifolds reach halfway to the crossing point while at the same time perturber character is redistributed from the location of the nominal perturber to nearby states. The effect is to halve the spacing between states and thus double the scaled action of the contributing orbits. This is the analog of the changing periodicity observed in Fig. 3. Above a scaled energy of  $-4$  the manifolds cross and strong recurrences ap-

pear with the same spacing seen at large-magnitude scaled energies. The perturber character again moves out from the nominal perturber location and back in between scaled energies of  $-12$  and  $-8$ , but all at modest manifold splitting. This gives rise to the increased decay of the recurrences seen at a scaled energy of  $-10$ .

## VI. CONCLUSION

The fundamental ideas behind closed-orbit theory appear universal. Studies on multi-electron systems test this. Our work has examined barium in a region where the configuration interaction is strong, but offers a simplification because only a modest range in energy is involved. This limits the resolution with which the system need be considered. We observe that the behavior of a wave packet in this system, though different from the one-electron case, can be related to it using a few simple ideas. There are also similarities between recurrence maps. We plan to turn to a search for the contributing closed orbits in the next phase of this work.

## ACKNOWLEDGMENTS

We thank J. B. Delos for valuable discussions. This research was supported by the National Science Foundation.

- 
- [1] See, for example, J. Main, G. Wiebusch, A. Holle, and K. Welge, *Phys. Rev. Lett.* **57**, 2789 (1986); U. Eichmann, K. Richter, D. Wintgen, and W. Sander, *ibid.* **61**, 2438 (1988); J.-M. Mao, K.A. Rapelje, S.J. Blodgett-Ford, J.B. Delos, A. König, and H. Rinneberg, *Phys. Rev. A* **48**, 2117 (1993); J. Main, G. Wiebusch, K. Welge, J. Shaw, and J.B. Delos, *ibid.* **49**, 847 (1994).
  - [2] For the Stark problem consider J. Gao and J.B. Delos, *Phys. Rev. A* **46**, 1455 (1992); J. Gao, J.B. Delos, and M. Baruch, *ibid.* **46**, 1449 (1992); J. Gao and J.B. Delos, *ibid.* **49**, 869 (1994).
  - [3] M. Courtney, N. Spellmeyer, H. Jiao, and D. Kleppner, *Phys. Rev. A* **51**, 3604 (1995).
  - [4] B. Hupper, J. Main, and G. Wunner, *Phys. Rev. Lett.* **74**, 2650 (1995).
  - [5] P.A. Dando, T.S. Monteiro, D. Delande, and K.T. Taylor, *Phys. Rev. Lett.* **74**, 1099 (1995).
  - [6] F. Robicheaux and J. Shaw, *Phys. Rev. A* **58**, 1043 (1998).
  - [7] B. Granger and C.H. Greene, *Phys. Rev. A* **62**, 012511 (2000).
  - [8] Y. Qiu, J. Müller, and J. Burgdörfer, *Phys. Rev. A* **54**, 1922 (1996).
  - [9] M. Keeler and T.J. Morgan, *Phys. Rev. Lett.* **80**, 5726 (1998).
  - [10] A. Kips, W. Vassen, W. Hogervorst, and P.A. Dando, *Phys. Rev. A* **58**, 3043 (1998).
  - [11] G.J. Kuik, A. Kips, W. Vassen and W. Hogervorst, *J. Phys. B* **29**, 2159 (1996).
  - [12] A. Kips, W. Vassen, and W. Hogervorst, *J. Phys. B* **33**, 109 (2000).
  - [13] J.G. Story, D.I. Duncan, and T.F. Gallagher, *Phys. Rev. Lett.* **71**, 3431 (1993); J.H. Hoogenraad, R.B. Vrijen, and L.D. Noordam, *Phys. Rev. A* **50**, 4133 (1994); D.W. Schumacher, D.I. Duncan, R.R. Jones, and T.F. Gallagher, *J. Phys. B* **29**, L397 (1996); D.W. Schumacher, B.J. Lyons, and T.F. Gallagher, *Phys. Rev. Lett.* **78**, 4359 (1997).
  - [14] J.A. Shaw and F. Robicheaux, *Phys. Rev. A* **58**, 1910 (1998).
  - [15] O. C. Mullins, Y. Zhu, and T.F. Gallagher, *Phys. Rev. A* **32**, 243 (1985).
  - [16] D.J. Armstrong, C.H. Greene, R.P. Wood, and J. Cooper, *Phys. Rev. Lett.* **70**, 2379 (1993).
  - [17] C. Westdorp, L.D. Noordam, and F. Robicheaux, *Phys. Rev. A* **60**, R3377 (1999).
  - [18] M.L. Zimmerman, T.W. Ducas, M.G. Littman, and D. Kleppner, *J. Phys. B* **11**, L11 (1978).
  - [19] L.D. Noordam, D.I. Duncan, and T.F. Gallagher, *Phys. Rev. A* **45**, 4734 (1992); R.R. Jones, D.W. Schumacher, T.F. Gallagher, and P.H. Bucksbaum, *J. Phys. B* **28**, L405 (1995).
  - [20] S.N. Pisharody, J.G. Zeibel, and R.R. Jones, *Phys. Rev. A* **61**, 063405 (2000).
  - [21] R.V. Jensen, H. Flores-Rueda, J.D. Wright, M.L. Keeler, and T.J. Morgan, *Phys. Rev. A* **62**, 053410 (2000).